

Uncertainty-o: One Model-agnostic Framework for Unveiling Uncertainty in Large Multimodal Models

Ruiyang Zhang¹ Hu Zhang² Hao Fei³ Zhedong Zheng^{1*}

¹ FST and ICI, University of Macau, China

² CSIRO Data61, Australia ³ National University of Singapore

Abstract

Large Multimodal Models (LMMs), harnessing the complementarity among diverse modalities, are often considered more robust than pure Language Large Models (LLMs); yet do LMMs know what they do not know? There are three key open questions remaining: (1) how to evaluate the uncertainty of diverse LMMs in a unified manner, (2) how to prompt LMMs to show its uncertainty, and (3) how to quantify uncertainty for downstream tasks.

In an attempt to address these challenges, we introduce **Uncertainty-o**: (1) a model-agnostic framework designed to reveal uncertainty in LMMs regardless of their modalities, architectures, or capabilities, (2) an empirical exploration of multimodal prompt perturbations to uncover LMM uncertainty, offering insights and findings, and (3) derive the formulation of multimodal semantic uncertainty, which enables quantifying uncertainty from multimodal responses. Experiments across 18 benchmarks spanning various modalities and 10 LMMs (both open- and closed-source) demonstrate the effectiveness of **Uncertainty-o** in reliably estimating LMM uncertainty, thereby enhancing downstream tasks such as hallucination detection, hallucination mitigation, and uncertainty-aware Chain-of-Thought reasoning.

1. Introduction

Large Multi-Modal Models (LMMs) [9, 11] significantly expand the boundaries of human-made intelligence. (1) **Rich modalities are continuously integrated.** Beyond the initial success of the ‘Text-in-Text-out’ paradigm [1], LMMs now incorporate images [46, 56], videos [43, 47], audio [39, 54], point clouds [50, 75], IMU [28], fMRI [30], and more [67]. (2) **Diverse model architectures are rapidly evolving.** The foundational designs of Large Language Models (LLMs) [1, 8] and Diffusion Models (DMs) [31, 56] have been extensively adapted [46] and in-

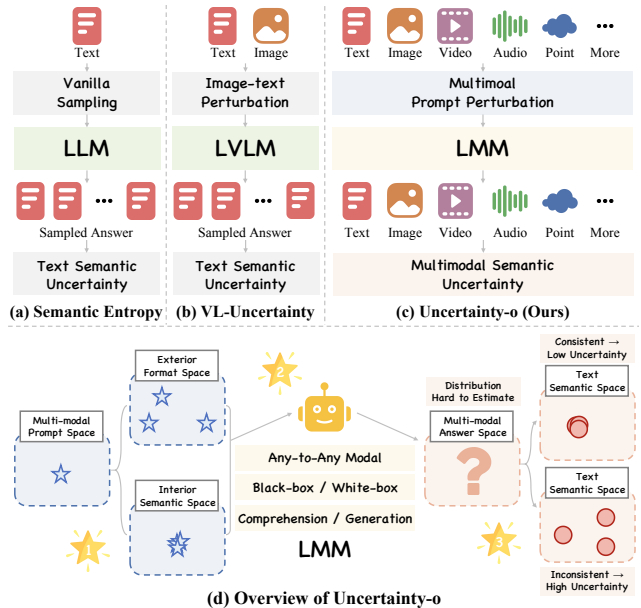


Figure 1. **Comparison with Previous Works and Overview of Uncertainty-o.** (a,b) Existing studies focus on single modality or two modalities [82]; (c) In contrast, our **Uncertainty-o** captures uncertainty in *large multimodal models* in a model-agnostic manner. It achieves reliable uncertainty estimation via *multimodal prompt perturbation*. (d) In particular, we harnessing *multimodal semantic uncertainty*, which maps multimodal answer space into a unified text semantic space. We then estimate the uncertainty according to the text consistency.

tegrated [68] to create more advanced and complex structures. (3) **Distinct model capabilities have significantly improved.** LMMs can now comprehend intricate multimodal contexts and instructions [30, 48], while simultaneously generating diverse and high-fidelity content [67, 78].

However, large models [1, 46] still follow a vanilla ‘Prompt-In-Response-Out’ pipeline, which remains raw and primitive compared to human thinking process [4, 52]. When asked a question or given a task, humans not only provide an answer or take action, but also experience internal feelings: confidence or uncertainty, ease or diffi-

*Correspondence to zhedongzheng@um.edu.mo.

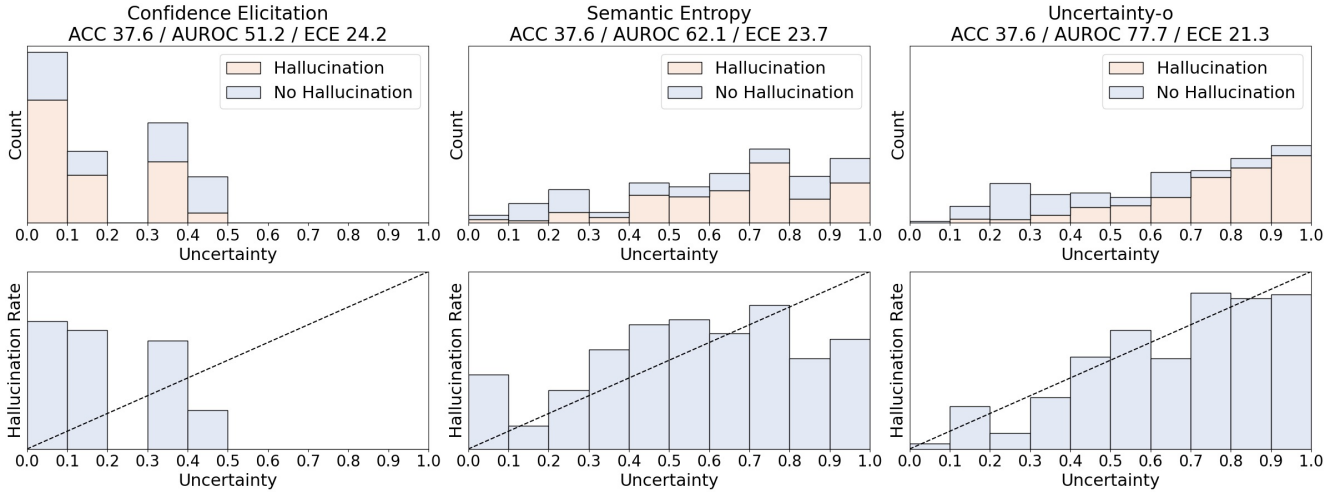


Figure 2. **Reliability of Our Estimated Uncertainty.** From comparison with previous methods, we observe that: (1) Compared to Confidence Elicitation [72], Uncertainty-o effectively avoids the over-confidence problem, which inaccurately assigns low uncertainty (or high confidence) to hallucinatory responses. (2) Compared to Semantic Entropy [24], Uncertainty-o provides more reliable uncertainty estimation, *e.g.*, the uncertainty is more closely aligned with the error rate in each bin. Results from OneLLM [30] on ClothV2 [21].

culty [18, 51]. These feelings guide us in predicting outcomes and adjusting our plans accordingly [5, 10]. To bridge this gap and explore the psychology of LMMs [29, 37], we focus on one critical property: LMM uncertainty [2, 57].

Despite the strong performance of LMMs, three key open questions remains: (1) **How to evaluate the uncertainty of diverse LMMs in a unified manner?** It is challenging in keeping the same evaluation standard for different LMMs. The vanilla solution is to design specific solutions according to the input modality, but can result in a complex and inflexible framework, limiting adaptability to involving new modalities [9, 11]. (2) **How to prompt LMM show its uncertainty?** The naive method is ask the LMM uncertainty via prompt inputs, but it usually fails. It is due to that LMMs, including LLMs, are usually over-confident about their response. (3) **How can we quantify uncertainty for downstream tasks?** The cues are embedded in multimodal responses [39, 50, 56, 67], *e.g.*, generated images [56] or point clouds [40], requiring effective techniques to extract and quantify LMM uncertainty to facilitate downstream tasks.

In response to those substantial questions, we propose Uncertainty-o (see Fig. 1): (1) **Uncertainty-o, in a model-agnostic manner, unveils uncertainty in LMMs, regardless of the modalities involved, inherent architecture, and capability focus.** Notably, Uncertainty-o is also scalable and can incorporate emerged modalities, architectures, and capabilities. (2) **We empirically explore multimodal prompt perturbation for revealing prompt aleatoric uncertainty.** By causing variance at the prompt end, we can observe fluctuations in LMM responses. Higher degree of fluctuation indicates higher level of aleatoric uncertainty, illustrating challenge and complexity of prompt. We provide a comprehensive empirical analysis of perturbation for

5 commonly used modalities, including text, image, video, audio, and point cloud. Finally, we offer our findings and insights, which are modality-agnostic and can serve as a cookbook when designing perturbation for other potential modalities. (3) **We propose multimodal semantic uncertainty, which can mine LMM inherent epistemic uncertainty from multimodal responses.** Through mapping multimodal responses to text semantic space, the observation of answer semantic distribution becomes addressable. The answer distribution entropy in the text semantic space serve as an effective indicator of epistemic uncertainty. Furthermore, uncertainties of each modality are merged to reveal overall LMM uncertainty.

Through extensive experiments with 18 multimodal benchmarks (including 5 modalities) and 10 LMMs (both open- and closed-source), we validate the effectiveness of Uncertainty-o in accurately capturing the uncertainty of LMMs. The reliable uncertainty estimation (see Fig. 2) facilitates various downstream tasks, including hallucination detection, hallucination mitigation, and uncertainty-aware CoT. In summary, our contributions are as follows:

- **Unified Framework to Unveil LMM Uncertainty.** We propose Uncertainty-o, which, in a model-agnostic manner, reveals one critical property in LMM psychology: uncertainty. Uncertainty-o can seamlessly handle LMMs with various modalities, complex model architectures, and distinct capacity emphases.
- **Cookbook for Multimodal Prompt Perturbation.** We propose multimodal prompt perturbation and empirically explore how to perturb the prompt to maximize its contribution to revealing prompt *aleatoric uncertainty*.
- **Multimodal Uncertainty in Semantic Space.** We propose multimodal semantic uncertainty, explicitly enabling the mining of inherent *epistemic uncertainty* from multimodal generated content via semantic space mapping.

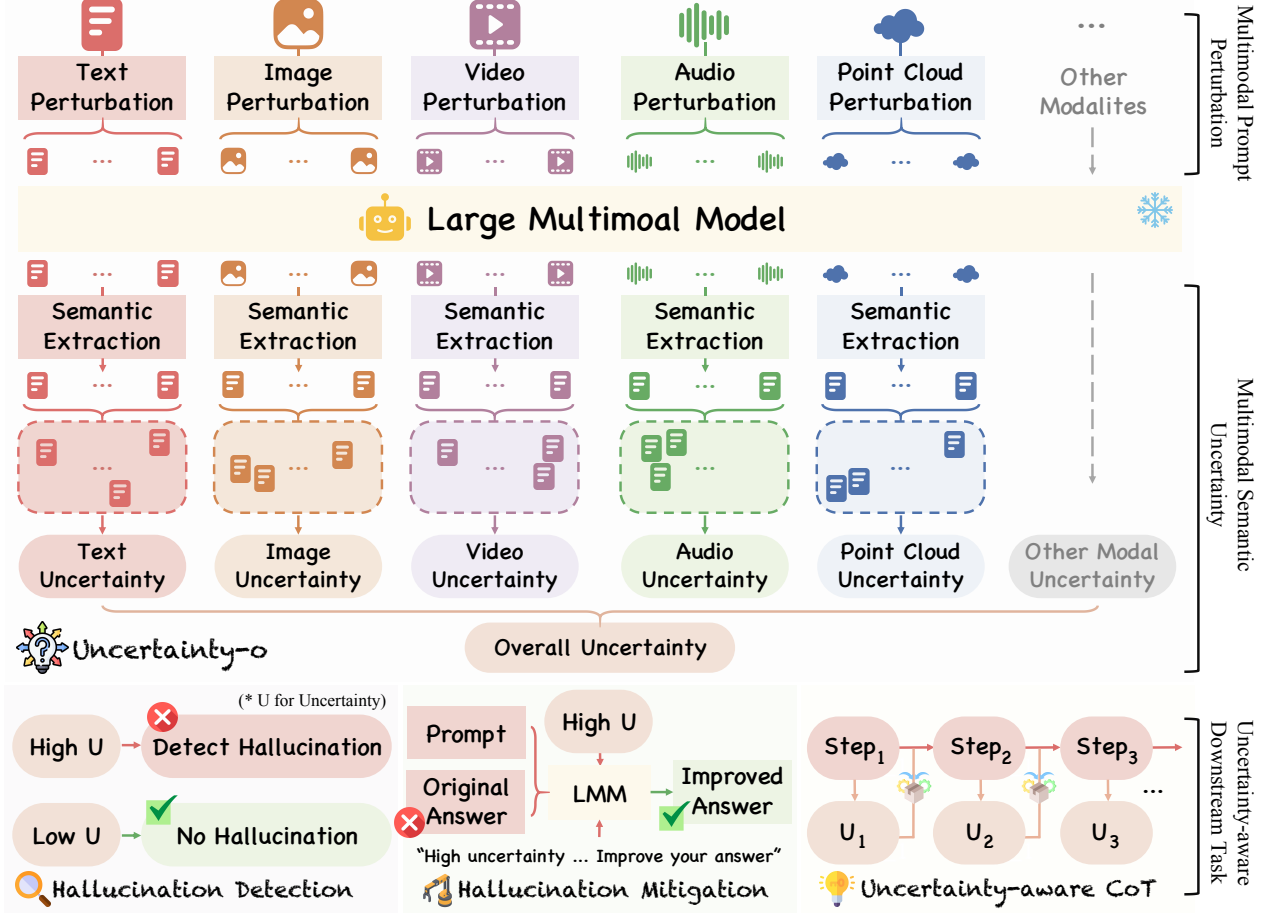


Figure 3. **Pipeline of Our Uncertainty-o.** Given a multimodal prompt and large multimodal models, we perform multimodal prompt perturbation to generate diverse responses. Due to the inherent epistemic uncertainty of these models under perturbation, varied responses are typically obtained. To quantify this uncertainty, we apply semantic clustering on the collected responses and compute their entropy. Specifically, responses are grouped into semantically similar clusters, and the entropy across these clusters is calculated as the final uncertainty measure. Higher entropy indicates greater variability in responses, suggesting lower confidence, while lower entropy reflects higher consistency and thus higher confidence. Finally, we could leverage the uncertainty for hallucination detection, hallucination mitigation and facilitate the chain of thoughts (CoT).

2. Uncertainty-o

2.1. Multimodal Prompt Perturbation

Definition 3.1 (Response Semantic Distance). The LMM M generate responses for prompts x_i and x_j (perturbed from original prompt x). For perturbed prompts, the predictions from LMM is $y_i = M(x_i)$, and $y_j = M(x_j)$, respectively. We focus on the LMM’s *Epistemic Uncertainty*, which is the uncertainty in the model parameters, $\text{Var}(\theta|x)$. Define the prediction difference $D(x)$ as:

$$D(x) = \|y_i - y_j\|, \quad (1)$$

where $\|\cdot\|$ denotes ℓ_2 norm.

Proposition 3.2. Response semantic distance $D(x)$ from prompt perturbation is proportional to the square root of

the LMM uncertainty:

$$D(x) \propto \sqrt{\text{Var}(\theta|x)}. \quad (2)$$

Therefore, the prediction semantic distance $D(x)$ can serve as a measure of the LMM uncertainty under given context.

Based on Proposition 3.2, we propose semantic-equivalent perturbation for multimodal prompts to induce variations in LMM responses, enabling the capture of LMM uncertainty (see Fig. 3). This approach generates semantic-equivalent variations of original prompts across multiple modalities and feeds them into the LLM. The variance in the sampled responses could effectively illustrate LMM uncertainty. Specifically, we propose multimodal prompt perturbation across five modalities, including text, image, audio, video, and point cloud. Notably, we adopt a progres-

sive perturbation strategy, where each prompt is gradually perturbed from low to high degrees, introducing increasing levels of challenge to the LMM. Perturbations across different modalities are applied simultaneously to further enhance uncertainty estimation.

In practice, different perturbation techniques are applied depending on the modality. For text prompts, both LLM-based rephrasing and rule-based methods, such as word swapping, are used. For image prompts, spatial transformations like rotation and attribute distortions such as blurring or brightness adjustments are applied. In the case of audio prompts, key elements like volume, pitch, and timbre are perturbed, with additional temporal adjustments such as temporal shifting. For video prompts, both spatial and temporal perturbations are applied. Temporal perturbations include techniques like temporal cropping and frame dropping, while spatial perturbations involve applying image perturbation techniques to each video frame. For point cloud prompts, 3D characteristics such as point density and shape are perturbed, using techniques like random sampling and point cloud jittering.

2.2. Multimodal Semantic Uncertainty

We quantify the variance of these sampled answers to capture the inherent uncertainty of the LMM. Instead of simply calculating variance based on format differences, we focus on variations in answer semantics. To estimate the variance of sampled answer semantics, the most critical procedure lies in semantic checking between two generated answers. Given this challenge, especially for higher-level modalities, *e.g.*, video, we propose utilizing an off-the-shelf LMM captioner to extract answer semantics and summarize the key points into text captions. Consequently, the challenging multimodal semantic checking is converted to the more manageable text semantic checking (see Fig. 3).

For those text captions, we directly prompt the LLM to iteratively check pairs of text answers. For texts with similar semantics, we cluster them into one group. After obtaining the semantic clusters of sampled answers, we analyze the discrete distribution of answer semantics and calculate the distribution entropy. Moreover, we normalize the calculated entropy compared to the maximum entropy decided by the sampling time, and obtain estimated LMM uncertainty, with higher values indicating greater LMM uncertainty:

$$u_m = - \sum_{i=1}^n p_i \log(p_i) \quad \text{where} \quad p_i = \frac{c_i}{C}, \quad (3)$$

where c_i is answer count for i -th group, C is the total answer count, u_m is the estimated uncertainty for certain modal m . Finally, uncertainties from all answer modalities is averaged to obtain final LMM uncertainty u .

2.3. Uncertainty-Aware Downstream Task

Hallucination Detection. We treat answers with low uncertainty as non-hallucinatory and those with high uncertainty as hallucinatory. In practice, we first infer LMM using the original prompt to obtain an initial answer. This answer is then compared with the ground truth to determine whether it contains hallucinations. Next, we apply the proposed multimodal prompt perturbation and multimodal semantic uncertainty to estimate LMM uncertainty for its initial answer. Finally, we evaluate the alignment between the estimated uncertainty and actual hallucination using 3 different metrics: Area under the Receiver Operating Characteristic Curve (AUROC) [24], Area under the ‘Rejection Accuracy’ Curve (AURAC) [24], and Expected Calibration Error (ECE) [72]. AUROC and AURAC focus on ranking ability (higher is better), while ECE measures calibration (lower is better).

Hallucination Mitigation. We formulate hallucination mitigation as an uncertainty-aware, two-stage revision process. In the first stage, we prompt the LMM to generate an initial answer, which is then assigned an uncertainty score estimated by Uncertainty-o. After constructing an answer pool with corresponding uncertainties, we select the top-K answers with the highest uncertainty scores, as these are the most likely to contain hallucinations. In the second stage, we refine these high-uncertainty answers by prompting the LMM with the original context, initial answer, and uncertainty score. We explicitly tell the LLM that its initial answer has a high uncertainty score and instruct it to revise the response due to a potential hallucination. The revised answer is then used as the LMM final output:

$$y_{\text{final}} = M(x', y_{\text{initial}}, u), \quad y_{\text{initial}} \in \mathbf{Y}, \quad (4)$$

where \mathbf{Y} contains selected answers with the highest uncertainty scores. x' , y_{initial} , and u refer to the updated prompt, initial answer, and estimated uncertainty, respectively. y_{final} is the revised answer. This iterative process helps the LLM refine its responses and improve accuracy.

Uncertainty-Aware Chain-of-Thought. We leverage Uncertainty-o to enhance the vanilla CoT process. Self-reflection is crucial for LMMs during CoT, and our estimated uncertainty serves as a guiding signal to trigger self-reflection. Specifically, at each reasoning step, in addition to generating responses, we also estimate answer uncertainty. In the subsequent step, we incorporate the previous answer and its uncertainty into the context, explicitly prompting LLM to reflect on its reasoning process when it finds uncertainty is high, as:

$$y_t, u_t = M(C_t), \quad C_{t+1} = C_t \cup \{y_t, u_t\}, \quad (5)$$

where y_t and u_t is answer and uncertainty, given the context C_t at step t . This uncertainty-aware procedure facilitates a more detailed and cautious reasoning process.

<i>Image Comprehension</i>									
Method	LLaVABench [46]			MMVet [77]			CoCoCap [13]		
	AUROC↑	AURAC↑	ECE↓	AUROC↑	AURAC↑	ECE↓	AUROC↑	AURAC↑	ECE↓
Confidence Elicitation [72]	54.0	78.1	11.3	52.3	55.8	13.1	51.2	71.0	23.1
GAVIE [45]	45.3	75.2	23.8	55.4	45.2	9.4	57.7	<u>79.6</u>	28.9
Semantic Entropy [24]	65.8	87.4	14.9	60.6	56.9	8.8	60.1	78.4	6.9
Uncertainty-o (ours)	68.0	91.3	10.1	63.5	66.4	8.2	65.5	82.5	5.9
<i>Video Comprehension</i>									
Method	MSRVTTQA [73]			MSVDQA [73]			NextQA [71]		
	AUROC↑	AURAC↑	ECE↓	AUROC↑	AURAC↑	ECE↓	AUROC↑	AURAC↑	ECE↓
Confidence Elicitation [72]	<u>53.5</u>	32.6	<u>12.2</u>	51.0	32.8	16.1	51.5	65.9	10.9
GAVIE [45]	50.1	33.9	18.2	39.6	30.1	20.5	47.4	60.8	11.4
Semantic Entropy [24]	51.6	<u>35.1</u>	14.7	47.1	32.7	18.6	<u>59.1</u>	62.4	12.6
Uncertainty-o (ours)	55.4	39.2	10.8	52.4	36.3	14.5	67.4	69.0	7.4
<i>Audio Comprehension</i>									
Method	ClothoV2 [21]			ClothoQA [44]			AudioCaps [38]		
	AUROC↑	AURAC↑	ECE↓	AUROC↑	AURAC↑	ECE↓	AUROC↑	AURAC↑	ECE↓
Confidence Elicitation [72]	51.2	34.1	24.2	49.2	43.5	29.0	50.9	30.2	18.6
GAVIE [45]	51.1	31.9	30.6	53.1	46.7	23.9	47.7	34.8	19.7
Semantic Entropy [24]	<u>62.1</u>	38.5	<u>23.7</u>	<u>56.7</u>	<u>50.2</u>	17.9	50.9	42.4	<u>16.1</u>
Uncertainty-o (ours)	77.7	44.1	21.3	68.1	51.0	17.7	56.7	46.6	12.4
<i>Point Cloud Comprehension</i>									
Method	ModelNet [70]			ShapeNet [12]			Objaverse [19]		
	AUROC↑	AURAC↑	ECE↓	AUROC↑	AURAC↑	ECE↓	AUROC↑	AURAC↑	ECE↓
Confidence Elicitation [72]	47.1	78.0	36.1	46.4	72.1	39.7	49.5	28.0	<u>23.1</u>
GAVIE [45]	46.0	<u>84.5</u>	43.5	51.1	<u>75.4</u>	37.5	49.8	35.1	29.4
Semantic Entropy [24]	<u>52.7</u>	79.2	<u>39.8</u>	<u>54.6</u>	<u>73.6</u>	<u>32.6</u>	<u>50.1</u>	<u>38.5</u>	26.0
Uncertainty-o (ours)	66.5	92.1	31.9	60.6	78.0	31.7	56.9	43.8	18.7

Table 1. **Comprehension Hallucination Detection Results.** Uncertainty-o consistently outperforms strong baselines by a clear margin in LMM comprehension hallucination detection. For LMMs, We utilize InternVL [16], VideoLLaMA [79], OneLLM [30], PointLLM [75] for image, video, audio, point cloud comprehension. The best results are in **bold**, and the second-best results are underlined.

Method	MMVet [77] w. GPT4o [34]		
	AUROC↑	AURAC↑	ECE↓
Confidence Elicitation [72]	<u>49.5</u>	<u>67.8</u>	11.7
GAVIE [45]	49.0	65.6	10.4
Semantic Entropy [24]	52.8	64.9	11.1
Uncertainty-o (ours)	56.1	75.8	8.6
Method	MSRVTTQA [73] w. QwenVLMMax [6]		
	AUROC↑	AURAC↑	ECE↓
Confidence Elicitation [72]	54.7	39.9	<u>11.5</u>
GAVIE [45]	55.9	40.1	15.6
Semantic Entropy [24]	<u>56.8</u>	41.5	12.8
Uncertainty-o (ours)	60.1	47.5	8.9

Table 2. **Hallucination Detection for Closed-Source LMMs.** We leverage GPT4o [34] and QwenVLMMax [6] for image and video comprehension respectively.

Method	<i>Medical Diagnosis</i>		
	AUROC↑	AURAC↑	ECE↓
Confidence Elicitation [72]	42.1	30.9	24.5
GAVIE [45]	44.2	33.6	31.5
Semantic Entropy [24]	<u>52.4</u>	<u>34.5</u>	<u>24.1</u>
Uncertainty-o (ours)	59.0	40.6	15.3
Method	<i>Embodied Robot</i>		
	AUROC↑	AURAC↑	ECE↓
Confidence Elicitation [72]	40.1	49.6	<u>18.9</u>
GAVIE [45]	45.2	53.6	23.5
Semantic Entropy [24]	<u>56.2</u>	<u>55.9</u>	21.1
Uncertainty-o (ours)	58.2	66.5	12.2

Table 3. **Hallucination Detection for Safety-Critic Tasks.** We harness MIMICXR [36] for medical image diagnosis and OpenEQ [49] for video embodied QA.

3. Experiment

3.1. Comparison with State-of-the-Arts

Comprehension Hallucination Detection. We compare Uncertainty-o with previous state-of-the-art methods in image, video, audio, and point cloud comprehension hallucination detection tasks (see Tab. 1). Uncertainty-o yields

significant and consistent performance improvements over strong baselines. This validates the general efficacy of the proposed multimodal prompt perturbation in better eliciting and capturing uncertainty, thereby facilitating reliable hallucination detection. Notably, Uncertainty-o surpasses baselines by 15.6% (AUROC) on ClothoV2, 9.5% (AURAC) on MMVet, 7.9% (ECE) on ModelNet, and 4.1% (AURAC) on NextQA. We also observe consistent improve-

Image Generation			
Method	Flickr [53]		ECE↓
	AUROC↑	AURAC↑	
GAVIE [45]	52.3	67.9	12.7
Semantic Entropy [24]	50.8	70.1	21.5
Uncertainty-o (ours)	59.5	74.5	8.3
Video Generation			
Method	MSRVTT [74]		ECE↓
	AUROC↑	AURAC↑	
GAVIE [45]	51.6	24.1	21.7
Semantic Entropy [24]	54.7	30.9	23.0
Uncertainty-o (ours)	61.1	38.9	15.5
Audio Generation			
Method	VCTK [76]		ECE↓
	AUROC↑	AURAC↑	
GAVIE [45]	46.0	74.6	21.5
Semantic Entropy [24]	48.1	72.8	20.6
Uncertainty-o (ours)	53.5	81.4	11.3
Point Cloud Generation			
Method	Pix3D [59]		ECE↓
	AUROC↑	AURAC↑	
GAVIE [45]	27.9	34.2	39.5
Semantic Entropy [24]	43.6	38.8	43.5
Uncertainty-o (ours)	51.1	44.2	32.0

Table 4. **Generation Hallucination Detection Results.** We utilize StableDiffusion [56], VideoFusion [47], AnyGPT [78], RGB2point [40] for image, video, audio, point cloud generation.

ment for closed-source LMMs, which validate the robustness of our Uncertainty-o (see Tab. 2). We further present a comparison of detection efficacy in the Medical Diagnosis and Embodied Robot domains (see Tab. 3). We observe that Uncertainty-o effectively handles complexity in real-world applications and outperforms baselines by clear margins.

Generation Hallucination Detection. We also present results on generation hallucination detection tasks across image, video, audio, and point cloud modalities (see Tab. 4). We adapt GAVIE [45] here and extend text-only semantic entropy in [24] with our multimodal semantic uncertainty. We observe that Uncertainty-o consistently shows clear improvements over these baselines. For example, we Uncertainty-o achieves 23.2% higher AUROC, 10% higher AURAC in the point cloud generation task. These results validate that the interaction between multimodal prompt perturbation and multimodal semantic uncertainty can effectively achieve more accurate hallucination detection.

Hallucination Mitigation. We report comprehension hallucination mitigation results on four video and audio benchmarks (see Tab. 5). “Direct inference” accuracy is the result without our proposed uncertainty and is reproduced by ourselves. With our uncertainty-guided revision process, we observe consistent accuracy improvement. These results validate the efficacy of our estimated uncertainty in benefiting the hallucination mitigation process.

Uncertainty-Aware CoT. We show the comparison between Uncertainty-Aware CoT and vanilla CoT (see Tab. 6).

Video Comprehension		
VideoLLaMA [79]	MSRVTTQA [73]	MSVDQA [73]
	Acc.	Acc.
Direct Inference	62.9	70.5
+ Uncertainty-o	67.2	72.1
Audio Comprehension		
OneLLM [30]	ClothoAQA [44]	ClothoV2 [21]
	Acc.	Acc.
Direct Inference	57.1	45.5
+ Uncertainty-o	59.2	51.9

Table 5. **Hallucination Mitigation Results.** Our uncertainty-guided revision effectively mitigates answer hallucination.

Image Comprehension		
InternVL [16]	MMVet [77]	LLaVABench [46]
	# Step	# Step
Vanilla CoT	3.1	2.6
Uncertainty-Aware CoT	5.4	4.1
Point Cloud Comprehension		
PointLLM [75]	ModelNet [70]	ShapeNet [12]
	# Step	# Step
Vanilla CoT	2.7	3.5
Uncertainty-Aware CoT	3.4	4.8

Table 6. **Uncertainty-Aware Chain-of-Thought Results.** Our estimated uncertainty enrich reasoning context, facilitating more thorough thinking process. We report average reasoning steps.

By incorporating uncertainty into the thinking context, LMMs generate a more comprehensive thinking process. On average, Uncertainty-Aware CoT leads to a noticeable increase in overall thinking length.

3.2. Ablation Studies and Further Discussions

Empirical Study on Multimodal Prompt Perturbation.

We present an empirical comparison of 24 different prompt perturbations for video, audio, and point cloud (see Fig. 4). For video perturbation, we find that perturbations that preserve the original video semantics, *e.g.*, adjust video speed, achieve superior results. In contrast, perturbations that alter the original semantics, *e.g.*, spatial cropping, lead to sub-optimal results due to over-estimated uncertainty. For audio perturbation, a similar pattern is observed. We observe that perturbations that preserve the original audio semantics contribute more to reliable uncertainty estimation, *e.g.*, adjusting volume. With the internal semantics intact and the external presentation changed, fluctuations in the sampled answers can directly reflect LMM uncertainty. For point cloud perturbation, a similar pattern also appears: operations that preserve the point cloud semantics are more beneficial for accurate hallucination detection.

Cookbook 1: Try to use perturbation that largely preserves original prompt semantic.

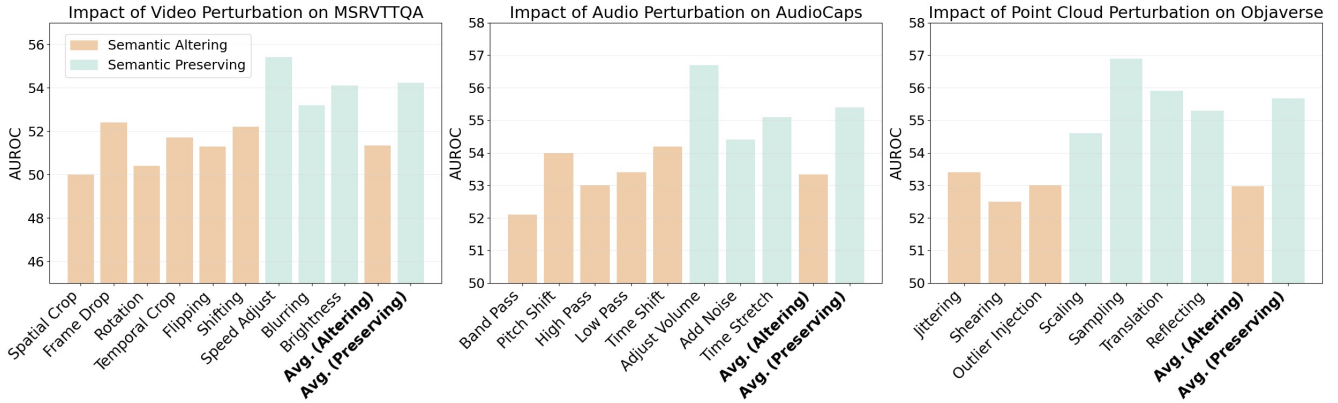


Figure 4. **Empirical Comparison of Different Prompt Perturbations.** On average, semantic-preserving perturbations are more effective for eliciting LMM uncertainty than semantic-altering ones. Results from comprehension hallucination detection for video, audio, point.

Text	Video	Audio	Point	AUROC \uparrow	AURAC \uparrow	ECE \downarrow
\times	\times	-	-	51.6	35.1	14.7
\checkmark	\times	-	-	53.0	36.1	13.9
\times	\checkmark	-	-	54.1	37.5	12.9
\checkmark	\checkmark	-	-	55.4	39.2	10.8
<hr/>						
\times	-	\times	-	50.9	42.4	16.1
\checkmark	-	\times	-	53.0	42.6	15.5
\times	-	\checkmark	-	52.6	44.9	12.9
\checkmark	-	\checkmark	-	56.7	46.6	12.4
<hr/>						
\times	-	-	\times	50.1	38.5	26.0
\checkmark	-	-	\times	52.4	40.2	20.9
\times	-	-	\checkmark	54.1	41.6	19.1
\checkmark	-	-	\checkmark	56.9	43.8	18.7

Table 7. **Ablation of Perturbation Combination.** We observe that combining perturbations for multimodal prompts yield better results. Single modal prompt perturbation could also yield performance improvements. Results from comprehension hallucination detection on MSRVTTQA [73], AudioCaps [38], and Objaverse [19]. Row with gray shading is our default setting.

Perturbation Combination. We report the ablation of perturbation combinations in Tab. 7. Concurrently perturbing multimodal prompts yields the best results. This approach effectively mines the uncertainty arising from each modality and contributes to capturing accurate LMM uncertainty.

Cookbook 2: Apply perturbation to prompt from different modalities simultaneously.

Pairing Order. We present an ablation of pairing order in Tab. 8. For multimodal prompts perturbed to various degrees, pairing them with a similar degree in a progressive manner yields the best results. This approach creates a prompt set with challenge levels from low to high, effectively eliciting LMM uncertainty.

Cookbook 3: Perturb prompts from each modality to varying degrees and pair them in the progressive order.

Pairing Order	AUROC \uparrow	AURAC \uparrow	ECE \downarrow
Progressive	55.4	39.2	10.8
Random	51.1	37.2	13.9
Shifted	52.4	37.8	12.5

Table 8. **Pairing Order for Perturbed Prompts.** Pairing prompts with similar degrees of perturbation from different modalities yields the best results. Results from comprehension hallucination detection on MSRVTTQA. Our default setting is in gray.

Sampling Time	AUROC \uparrow	AURAC \uparrow	ECE \downarrow
2	50.6	35.1	15.9
3	54.2	36.9	12.4
5	55.4	39.2	10.8
8	55.1	38.9	11.6
10	54.9	39.2	11.2

Table 9. **Ablation of Sampling Time.** Moderate sampling time enables the most effective uncertainty estimation. We report MSRVTTQA comprehension hallucination detection results. Our default setting is highlighted with gray shading.

Sampling Time. We illustrate the ablation of sampling time during the uncertainty estimation process (see Tab. 9). With a moderate sampling time, *e.g.*, 5 times, we achieve optimal results. A sampling time that is too small fails to effectively model LMM uncertainty, while excessively high sampling times inevitably lead to over-estimated uncertainty.

Cookbook 4: Try with a moderate perturbation time (sampling time), *e.g.*, 5 times.

Qualitative Results of Successful Hallucination Detection. We present successful hallucination detection cases for both comprehension and generation scenarios in Fig. 5. With the proposed multimodal prompt perturbation, Uncertainty-o achieves reliable uncertainty estimation, leading to accurate hallucination detection.

4. Related Work

Large Multimodal Model. Large Multimodal Models (LMMs) [9] perceive and generate content across a wide

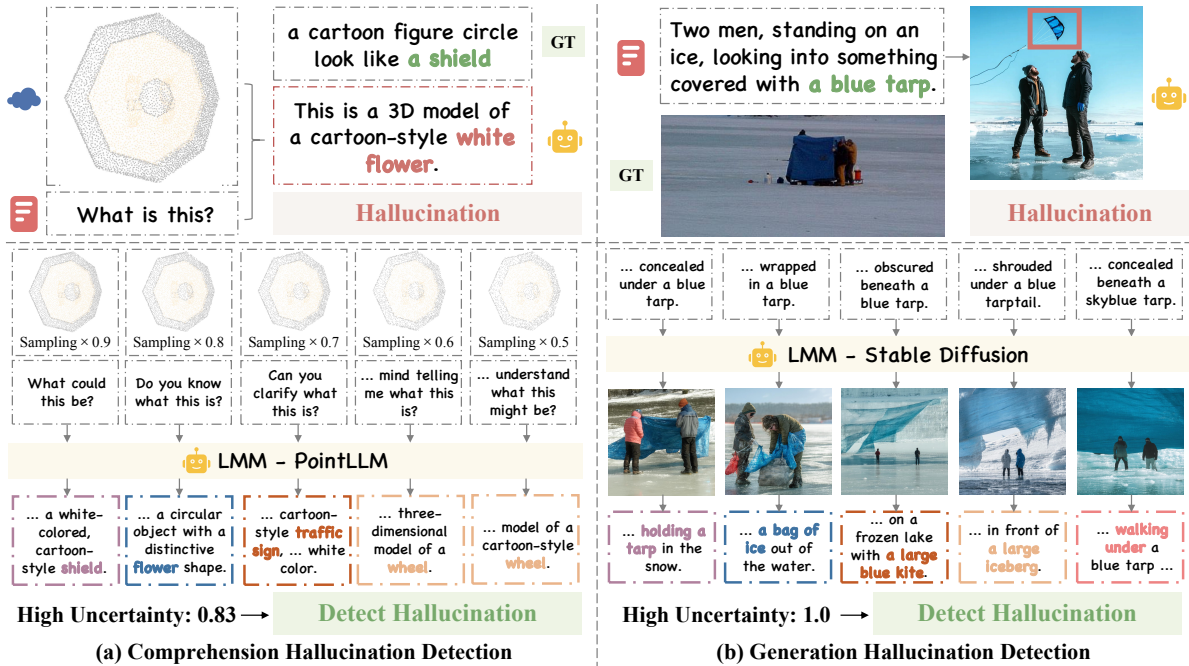


Figure 5. **Qualitative Results of Successful Hallucination Detection.** Uncertainty-o is proficient at accurately detecting multiple hallucinations, including comprehension (point cloud QA [19]) and generation tasks (image generation [53]) based on the uncertainty value.

range of modalities [9, 65, 80, 81], such as text [1], image [26, 56], audio [78], video [25, 47], point cloud [75], and more. Fundamental efforts pioneer in building a universal-modal encoder by aligning various modalities to language [28, 48]. On one hand, various works [30, 43, 46, 75] focus on enhancing multimodal comprehension ability [27], emphasizing the understanding of complexity [66] and interaction [83] between prompts from various modalities [69]. Another line of research focuses on generating multimodal content [40, 47, 56, 78], with an emphasis on the fidelity [41, 58] and diversity [22, 62] of multimodal responses. Moreover, recent works [67, 78] try to build ‘Any-to-Any’ capability [60, 61] in large models, where models can simultaneously comprehend complex contexts and generate high-fidelity content following those contexts.

LMM Hallucination Detection. LMM Hallucination Detection [7, 33] aims for detecting either context-misfollowing [32] or factual mistakes [3] in generated multimodal responses. For external-evaluator-based approaches, powerful response scorers [45, 63] or retrieved real-world fact [14, 20] facilitate hallucination detection. For discrete rule-based checking, CHAIR [55] employs the ratio of objects presented in the response relative to a ground truth object list to identify hallucinatory answers, which is limited to fixed object classes. Building on CHAIR, POPE [42] enhances the prompting technique by focusing on Yes-or-No questions, simplifying process and improving stability. Distinct from existing works, Uncertainty-o harnesses LMM uncertainty as intrinsic indicator of hallucination responses.

Uncertainty in LLM. MAP [35] proposes a proba-

bilistic distribution encoder to model uncertainty during large model pretraining. VL-Uncertainty [82] leverages semantic-equivalent perturbations of visual and textual prompts to better capture MLLM uncertainty. DropoutDecoding [23] treats token distribution discrepancies from the average token distribution as uncertainty, dropping tokens with high uncertainty. Calibration-MLLM [15] utilizes calibration between different stages of MLLM, such as before and after visual fine-tuning, to reveal uncertainty. IDK [17] introduces an additional special ‘I Don’t Know’ token, and quantify uncertainty based on predicted probability of this token. UAL [64] utilizes uncertainty for large model alignment and improves token convergence in feature space.

5. Conclusion

In this paper, we study LLMs reliability and explore the intrinsic uncertainty in LLMs. We propose Uncertainty-o, a model-agnostic framework that unveils uncertainty in LLMs and simultaneously processes five different modalities (visual, auditory, textual, video, and point clouds). Specifically, we first introduce multimodal prompt perturbation and empirically demonstrate that semantic-preserving perturbations are more effective for capturing LLM uncertainty. Then, we introduce multimodal semantic uncertainty based on the imposed perturbations, effectively mining uncertainty from multimodal generated responses. Extensive experiments and analysis validate superiority of Uncertainty-o in accurately estimating LLM uncertainty and facilitating various downstream tasks.

References

- [1] Josh Achiam, Steven Adler, Sandhini Agarwal, Lama Ahmad, Ilge Akkaya, Florencia Leoni Aleman, Diogo Almeida, Janko Altenschmidt, Sam Altman, Shyamal Anadkat, et al. Gpt-4 technical report. *arXiv:2303.08774*, 2023. 1, 8
- [2] Lukas Aichberger, Kajetan Schweighofer, Mykyta Ielanskyi, and Sepp Hochreiter. How many opinions does your llm have? improving uncertainty estimation in nlg. In *ICLR 2024 Workshop on Secure and Trustworthy Large Language Models*, 2024. 2
- [3] Mubashara Akhtar, Michael Schlichtkrull, Zhijiang Guo, Oana Cocarascu, Elena Simperl, and Andreas Vlachos. Multimodal automated fact-checking: A survey. *arXiv:2305.13507*, 2023. 8
- [4] Alfonso Amayuelas, Kyle Wong, Liangming Pan, Wenhui Chen, and William Wang. Knowledge of knowledge: Exploring known-unknowns uncertainty with large language models. *arXiv:2305.13712*, 2023. 1
- [5] Fabrizia Auletta, Rachel W Kallen, Mario di Bernardo, and Michael J Richardson. Predicting and understanding human action decisions during skillful joint-action using supervised machine learning and explainable-ai. *Scientific Reports*, 13(1):4992, 2023. 2
- [6] Jinze Bai, Shuai Bai, Shusheng Yang, Shijie Wang, Sinan Tan, Peng Wang, Junyang Lin, Chang Zhou, and Jingren Zhou. Qwen-vl: A versatile vision-language model for understanding, localization, text reading, and beyond, 2023. 5
- [7] Zechen Bai, Pichao Wang, Tianjun Xiao, Tong He, Zongbo Han, Zheng Zhang, and Mike Zheng Shou. Hallucination of multimodal large language models: A survey. *arXiv:2404.18930*, 2024. 8
- [8] Tom Brown, Benjamin Mann, Nick Ryder, Melanie Subbiah, Jared D Kaplan, Prafulla Dhariwal, Arvind Neelakantan, Pranav Shyam, Girish Sastry, Amanda Askell, et al. Language models are few-shot learners. *Advances in neural information processing systems*, 33:1877–1901, 2020. 1
- [9] Davide Caffagni, Federico Cocchi, Luca Barsellotti, Nicholas Moratelli, Sara Sarto, Lorenzo Baraldi, Marcella Cornia, and Rita Cucchiara. The revolution of multimodal large language models: a survey. *arXiv:2402.12451*, 2024. 1, 2, 7, 8
- [10] Frederick Callaway, Bas van Opheusden, Sayan Gul, Priyam Das, Paul M Krueger, Thomas L Griffiths, and Falk Lieder. Rational use of cognitive resources in human planning. *Nature Human Behaviour*, 6(8):1112–1125, 2022. 2
- [11] Kilian Carolan, Laura Fennelly, and Alan F Smeaton. A review of multi-modal large language and vision models. *arXiv:2404.01322*, 2024. 1, 2
- [12] Angel X Chang, Thomas Funkhouser, Leonidas Guibas, Pat Hanrahan, Qixing Huang, Zimo Li, Silvio Savarese, Manolis Savva, Shuran Song, Hao Su, et al. Shapenet: An information-rich 3d model repository. *arXiv:1512.03012*, 2015. 5, 6
- [13] Xinlei Chen, Hao Fang, Tsung-Yi Lin, Ramakrishna Vedantam, Saurabh Gupta, Piotr Dollár, and C Lawrence Zitnick. Microsoft coco captions: Data collection and evaluation server. *arXiv preprint arXiv:1504.00325*, 2015. 5
- [14] Xiang Chen, Chenxi Wang, Yida Xue, Ningyu Zhang, Xiaoyan Yang, Qiang Li, Yue Shen, Lei Liang, Jinjie Gu, and Huajun Chen. Unified hallucination detection for multimodal large language models. *arXiv:2402.03190*, 2024. 8
- [15] Zijun Chen, Wenbo Hu, Guande He, Zhijie Deng, Zheng Zhang, and Richang Hong. Unveiling uncertainty: A deep dive into calibration and performance of multimodal large language models. *arXiv:2412.14660*, 2024. 8
- [16] Zhe Chen, Jiannan Wu, Wenhui Wang, Weijie Su, Guo Chen, Sen Xing, Muyan Zhong, Qinglong Zhang, Xizhou Zhu, Lewei Lu, et al. Internvl: Scaling up vision foundation models and aligning for generic visual-linguistic tasks. In *Proceedings of the IEEE/CVF conference on computer vision and pattern recognition*, pages 24185–24198, 2024. 5, 6
- [17] Roi Cohen, Konstantin Dobler, Eden Biran, and Gerard de Melo. I don't know: Explicit modeling of uncertainty with an [jdk] token. *Advances in Neural Information Processing Systems*, 37:10935–10958, 2024. 8
- [18] Katherine Maeve Collins, Matthew Barker, Mateo Espinosa Zarlenga, Naveen Raman, Umang Bhatt, Mateja Jamnik, Ilija Sucholutsky, Adrian Weller, and Krishnamurthy Dvijotham. Human uncertainty in concept-based ai systems. In *Proceedings of the 2023 AAAI/ACM Conference on AI, Ethics, and Society*, pages 869–889, 2023. 2
- [19] Matt Deitke, Dustin Schwenk, Jordi Salvador, Luca Weihs, Oscar Michel, Eli VanderBilt, Ludwig Schmidt, Kiana Ehsani, Aniruddha Kembhavi, and Ali Farhadi. Objaverse: A universe of annotated 3d objects. In *CVPR*, pages 13142–13153, 2023. 5, 7, 8
- [20] Hanxing Ding, Liang Pang, Zihao Wei, Huawei Shen, and Xueqi Cheng. Retrieve only when it needs: Adaptive retrieval augmentation for hallucination mitigation in large language models. *arXiv:2402.10612*, 2024. 8
- [21] Konstantinos Drossos, Samuel Lipping, and Tuomas Virtanen. Clotho: An audio captioning dataset. In *ICASSP 2020-2020 IEEE International Conference on Acoustics, Speech and Signal Processing (ICASSP)*, pages 736–740. IEEE, 2020. 2, 5, 6
- [22] Rongyao Fang, Chengqi Duan, Kun Wang, Hao Li, Hao Tian, Xingyu Zeng, Rui Zhao, Jifeng Dai, Hongsheng Li, and Xihui Liu. Puma: Empowering unified mllm with multi-granular visual generation. *arXiv:2410.13861*, 2024. 8
- [23] Yixiong Fang, Ziran Yang, Zhaorun Chen, Zhuokai Zhao, and Jiawei Zhou. From uncertainty to trust: Enhancing reliability in vision-language models with uncertainty-guided dropout decoding. *arXiv:2412.06474*, 2024. 8
- [24] Sebastian Farquhar, Jannik Kossen, Lorenz Kuhn, and Yarin Gal. Detecting hallucinations in large language models using semantic entropy. *Nature*, 630(8017):625–630, 2024. 2, 4, 5, 6
- [25] Hao Fei, Shengqiong Wu, Wei Ji, Hanwang Zhang, Meishan Zhang, Mong-Li Lee, and Wynne Hsu. Video-of-thought: Step-by-step video reasoning from perception to cognition. *arXiv preprint arXiv:2501.03230*, 2024. 8
- [26] Hao Fei, Shengqiong Wu, Hanwang Zhang, Tat-Seng Chua, and Shuicheng Yan. Vitron: A unified pixel-level vision llm for understanding, generating, segmenting, editing. *arXiv preprint arXiv:2412.19806*, 2024. 8

- [27] Hao Fei, Shengqiong Wu, Meishan Zhang, Min Zhang, Tat-Seng Chua, and Shuicheng Yan. Enhancing video-language representations with structural spatio-temporal alignment. *IEEE Transactions on Pattern Analysis and Machine Intelligence*, 2024. 8
- [28] Rohit Girdhar, Alaaeldin El-Nouby, Zhuang Liu, Mannat Singh, Kalyan Vasudev Alwala, Armand Joulin, and Ishan Misra. Imagebind: One embedding space to bind them all. In *CVPR*, pages 15180–15190, 2023. 1, 8
- [29] Lewis Griffin, Bennett Kleinberg, Maximilian Mozes, Kimberly Mai, Maria Do Mar Vau, Matthew Caldwell, and Augustine Mavor-Parker. Large language models respond to influence like humans. In *Proceedings of the First Workshop on Social Influence in Conversations (SICoN 2023)*, pages 15–24, 2023. 2
- [30] Jiaming Han, Kaixiong Gong, Yiyuan Zhang, Jiaqi Wang, Kaipeng Zhang, Dahua Lin, Yu Qiao, Peng Gao, and Xianguy Yue. Onellm: One framework to align all modalities with language. In *CVPR*, pages 26584–26595, 2024. 1, 2, 5, 6, 8
- [31] Jonathan Ho, Ajay Jain, and Pieter Abbeel. Denoising diffusion probabilistic models. *Advances in neural information processing systems*, 33:6840–6851, 2020. 1
- [32] Jiaxing Huang and Jingyi Zhang. A survey on evaluation of multimodal large language models. *arXiv:2408.15769*, 2024. 8
- [33] Wen Huang, Hongbin Liu, Minxin Guo, and Neil Zhenqiang Gong. Visual hallucinations of multi-modal large language models. *arXiv:2402.14683*, 2024. 8
- [34] Aaron Hurst, Adam Lerer, Adam P Goucher, Adam Perelman, Aditya Ramesh, Aidan Clark, AJ Ostrow, Akila Welihinda, Alan Hayes, Alec Radford, et al. Gpt-4o system card. *arXiv preprint arXiv:2410.21276*, 2024. 5
- [35] Yatai Ji, Junjie Wang, Yuan Gong, Lin Zhang, Yanru Zhu, Hongfa Wang, Jiaying Zhang, Tetsuya Sakai, and Yujiu Yang. Map: Multimodal uncertainty-aware vision-language pre-training model. *arXiv:2210.05335*, 2022. 8
- [36] Alistair EW Johnson, Tom J Pollard, Seth J Berkowitz, Nathaniel R Greenbaum, Matthew P Lungren, Chih-ying Deng, Roger G Mark, and Steven Horng. Mimic-cxr, a de-identified publicly available database of chest radiographs with free-text reports. *Scientific data*, 6(1):317, 2019. 5
- [37] Luoma Ke, Song Tong, Peng Cheng, and Kaiping Peng. Exploring the frontiers of llms in psychological applications: A comprehensive review. *arXiv:2401.01519*, 2024. 2
- [38] Chris Dongjoo Kim, Byeongchang Kim, Hyunmin Lee, and Gunhee Kim. Audiocaps: Generating captions for audios in the wild. In *Proceedings of the 2019 Conference of the North American Chapter of the Association for Computational Linguistics: Human Language Technologies, Volume 1 (Long and Short Papers)*, pages 119–132, 2019. 5, 7
- [39] Felix Kreuk, Gabriel Synnaeve, Adam Polyak, Uriel Singer, Alexandre Défossez, Jade Copet, Devi Parikh, Yaniv Taigman, and Yossi Adi. Audiogen: Textually guided audio generation. *arXiv:2209.15352*, 2022. 1, 2
- [40] Jae Joong Lee and Bedrich Benes. Rgb2point: 3d point cloud generation from single rgb images. *arXiv:2407.14979*, 2024. 2, 6, 8
- [41] Wei Li, Xue Xu, Jiachen Liu, and Xinyan Xiao. Unimog: Unified image generation through multimodal conditional diffusion. *arXiv:2401.13388*, 2024. 8
- [42] Yifan Li, Yifan Du, Kun Zhou, Jinpeng Wang, Wayne Xin Zhao, and Ji-Rong Wen. Evaluating object hallucination in large vision-language models. *arXiv:2305.10355*, 2023. 8
- [43] Bin Lin, Yang Ye, Bin Zhu, Jiaxi Cui, Munan Ning, Peng Jin, and Li Yuan. Video-llava: Learning united visual representation by alignment before projection. *arXiv:2311.10122*, 2023. 1, 8
- [44] Samuel Lipping, Parthasaarathy Sudarsanam, Konstantinos Drossos, and Tuomas Virtanen. Clotho-aqa: A crowd-sourced dataset for audio question answering. In *2022 30th European Signal Processing Conference (EUSIPCO)*, pages 1140–1144. IEEE, 2022. 5, 6
- [45] Fuxiao Liu, Kevin Lin, Linjie Li, Jianfeng Wang, Yaser Yacoob, and Lijuan Wang. Mitigating hallucination in large multi-modal models via robust instruction tuning. *arXiv:2306.14565*, 2023. 5, 6, 8
- [46] Haotian Liu, Chunyuan Li, Qingyang Wu, and Yong Jae Lee. Visual instruction tuning. *NeurIPS*, 36:34892–34916, 2023. 1, 5, 6, 8
- [47] Zhengxiong Luo, Dayou Chen, Yingya Zhang, Yan Huang, Liang Wang, Yujun Shen, Deli Zhao, Jingren Zhou, and Tieniu Tan. Videofusion: Decomposed diffusion models for high-quality video generation. *arXiv:2303.08320*, 2023. 1, 6, 8
- [48] Yuanhuiyi Lyu, Xu Zheng, Jiazhou Zhou, and Lin Wang. Unibind: Llm-augmented unified and balanced representation space to bind them all. In *CVPR*, pages 26752–26762, 2024. 1, 8
- [49] Arjun Majumdar, Anurag Ajay, Xiaohan Zhang, Pranav Putta, Sriram Yenamandra, Mikael Henaff, Sneha Silwal, Paul Mcvay, Oleksandr Maksymets, Sergio Arnaud, et al. Openeqa: Embodied question answering in the era of foundation models. In *CVPR*, pages 16488–16498, 2024. 5
- [50] Alex Nichol, Heewoo Jun, Prafulla Dhariwal, Pamela Mishkin, and Mark Chen. Point-e: A system for generating 3d point clouds from complex prompts. *arXiv:2212.08751*, 2022. 1, 2
- [51] Joshua C Peterson, Ruairidh M Battleday, Thomas L Griffiths, and Olga Russakovsky. Human uncertainty makes classification more robust. In *ICCV*, pages 9617–9626, 2019. 2
- [52] Renjie Pi, Tianyang Han, Jianshu Zhang, Yueqi Xie, Rui Pan, Qing Lian, Hanze Dong, Jipeng Zhang, and Tong Zhang. Mllm-protector: Ensuring mllm’s safety without hurting performance. *arXiv:2401.02906*, 2024. 1
- [53] Bryan A Plummer, Liwei Wang, Chris M Cervantes, Juan C Caicedo, Julia Hockenmaier, and Svetlana Lazebnik. Flickr30k entities: Collecting region-to-phrase correspondences for richer image-to-sentence models. In *ICCV*, pages 2641–2649, 2015. 6, 8
- [54] Alec Radford, Jong Wook Kim, Tao Xu, Greg Brockman, Christine McLeavey, and Ilya Sutskever. Robust speech recognition via large-scale weak supervision. In *ICML*, pages 28492–28518. PMLR, 2023. 1

- [55] Anna Rohrbach, Lisa Anne Hendricks, Kaylee Burns, Trevor Darrell, and Kate Saenko. Object hallucination in image captioning. *arXiv:1809.02156*, 2018. 8
- [56] Robin Rombach, Andreas Blattmann, Dominik Lorenz, Patrick Esser, and Björn Ommer. High-resolution image synthesis with latent diffusion models. In *CVPR*, pages 10684–10695, 2022. 1, 2, 6, 8
- [57] Ola Shorinwa, Zhiting Mei, Justin Lidard, Allen Z Ren, and Anirudha Majumdar. A survey on uncertainty quantification of large language models: Taxonomy, open research challenges, and future directions. *arXiv:2412.05563*, 2024. 2
- [58] Kunpeng Song, Yizhe Zhu, Bingchen Liu, Qing Yan, Ahmed Elgammal, and Xiao Yang. Moma: Multimodal llm adapter for fast personalized image generation. In *ECCV*, pages 117–132, 2024. 8
- [59] Xingyuan Sun, Jiajun Wu, Xiuming Zhang, Zhoutong Zhang, Chengkai Zhang, Tianfan Xue, Joshua B Tenenbaum, and William T Freeman. Pix3d: Dataset and methods for single-image 3d shape modeling. In *CVPR*, pages 2974–2983, 2018. 6
- [60] Zineng Tang, Ziyi Yang, Chenguang Zhu, Michael Zeng, and Mohit Bansal. Any-to-any generation via composable diffusion. *Advances in Neural Information Processing Systems*, 36:16083–16099, 2023. 8
- [61] Zineng Tang, Ziyi Yang, Mahmoud Khademi, Yang Liu, Chenguang Zhu, and Mohit Bansal. Codi-2: In-context interleaved and interactive any-to-any generation. In *CVPR*, pages 27425–27434, 2024. 8
- [62] Guy Tevet and Jonathan Berant. Evaluating the evaluation of diversity in natural language generation. *arXiv:2004.02990*, 2020. 8
- [63] Junyang Wang, Yiyang Zhou, Guohai Xu, Pengcheng Shi, Chenlin Zhao, Haiyang Xu, Qinghao Ye, Ming Yan, Ji Zhang, Jihua Zhu, et al. Evaluation and analysis of hallucination in large vision-language models. *arXiv:2308.15126*, 2023. 8
- [64] Yikun Wang, Rui Zheng, Liang Ding, Qi Zhang, Dahua Lin, and Dacheng Tao. Uncertainty aware learning for language model alignment. *arXiv:2406.04854*, 2024. 8
- [65] Jiayang Wu, Wensheng Gan, Zefeng Chen, Shicheng Wan, and S Yu Philip. Multimodal large language models: A survey. In *2023 IEEE International Conference on Big Data (BigData)*, pages 2247–2256. IEEE, 2023. 8
- [66] Junda Wu, Zhehao Zhang, Yu Xia, Xintong Li, Zhaoyang Xia, Aaron Chang, Tong Yu, Sungchul Kim, Ryan A Rossi, Ruiyi Zhang, et al. Visual prompting in multimodal large language models: A survey. *arXiv:2409.15310*, 2024. 8
- [67] Shengqiong Wu, Hao Fei, Leigang Qu, Wei Ji, and Tat-Seng Chua. Next-gpt: Any-to-any multimodal llm. In *ICML*, 2024. 1, 2, 8
- [68] Tsung-Han Wu, Long Lian, Joseph E Gonzalez, Boyi Li, and Trevor Darrell. Self-correcting llm-controlled diffusion models. In *CVPR*, pages 6327–6336, 2024. 1
- [69] Xixi Wu, Yifei Shen, Caihua Shan, Kaitao Song, Siwei Wang, Bohang Zhang, Jiarui Feng, Hong Cheng, Wei Chen, Yun Xiong, et al. Can graph learning improve planning in llm-based agents? In *The Thirty-eighth Annual Conference on Neural Information Processing Systems*, 2024. 8
- [70] Zhirong Wu, Shuran Song, Aditya Khosla, Fisher Yu, Linguang Zhang, Xiaoou Tang, and Jianxiong Xiao. 3d shapenets: A deep representation for volumetric shapes. In *CVPR*, pages 1912–1920, 2015. 5, 6
- [71] Junbin Xiao, Xindi Shang, Angela Yao, and Tat-Seng Chua. Next-qa: Next phase of question-answering to explaining temporal actions. In *CVPR*, pages 9777–9786, 2021. 5
- [72] Miao Xiong, Zhiyuan Hu, Xinyang Lu, Yifei Li, Jie Fu, Junxian He, and Bryan Hooi. Can llms express their uncertainty? an empirical evaluation of confidence elicitation in llms. *arXiv:2306.13063*, 2023. 2, 4, 5
- [73] Dejing Xu, Zhou Zhao, Jun Xiao, Fei Wu, Hanwang Zhang, Xiangnan He, and Yueting Zhuang. Video question answering via gradually refined attention over appearance and motion. In *Proceedings of the 25th ACM international conference on Multimedia*, pages 1645–1653, 2017. 5, 6, 7
- [74] Jun Xu, Tao Mei, Ting Yao, and Yong Rui. Msr-vtt: A large video description dataset for bridging video and language. In *CVPR*, pages 5288–5296, 2016. 6
- [75] Runsen Xu, Xiaolong Wang, Tai Wang, Yilun Chen, Jiangmiao Pang, and Dahua Lin. Pointllm: Empowering large language models to understand point clouds. In *ECCV*, pages 131–147, 2024. 1, 5, 6, 8
- [76] Junichi Yamagishi, Christophe Veaux, and Kirsten MacDonald. Cstr vctk corpus: English multi-speaker corpus for cstr voice cloning toolkit (version 0.92). 2019. 6
- [77] Weihao Yu, Zhengyuan Yang, Linjie Li, Jianfeng Wang, Kevin Lin, Zicheng Liu, Xinchao Wang, and Lijuan Wang. Mm-vet: Evaluating large multimodal models for integrated capabilities. *arXiv:2308.02490*, 2023. 5, 6
- [78] Jun Zhan, Junqi Dai, Jiasheng Ye, Yunhua Zhou, Dong Zhang, Zhigeng Liu, Xin Zhang, Ruibin Yuan, Ge Zhang, Linyang Li, et al. Anygpt: Unified multimodal llm with discrete sequence modeling. *arXiv:2402.12226*, 2024. 1, 6, 8
- [79] Hang Zhang, Xin Li, and Lidong Bing. Video-llama: An instruction-tuned audio-visual language model for video understanding. *arXiv preprint arXiv:2306.02858*, 2023. 5, 6
- [80] Ruiyang Zhang, Hu Zhang, Hang Yu, and Zhedong Zheng. Approaching outside: scaling unsupervised 3d object detection from 2d scene. In *ECCV*, pages 249–266, 2024. 8
- [81] Ruiyang Zhang, Hu Zhang, Hang Yu, and Zhedong Zheng. Harnessing uncertainty-aware bounding boxes for unsupervised 3d object detection. *arXiv:2408.00619*, 2024. 8
- [82] Ruiyang Zhang, Hu Zhang, and Zhedong Zheng. VI-uncertainty: Detecting hallucination in large vision-language model via uncertainty estimation. *arXiv:2411.11919*, 2024. 1, 8
- [83] Yuechen Zhang, Shengju Qian, Bohao Peng, Shu Liu, and Jiaya Jia. Prompt highlighter: Interactive control for multimodal llms. In *CVPR*, pages 13215–13224, 2024. 8

Uncertainty-o: One Model-agnostic Framework for Unveiling Uncertainty in Large Multimodal Models

Supplementary Material

6. Discussion

Why is semantic-equivalent perturbation more effective than inequivalent perturbation? In semantic-equivalent perturbation, the semantics of all perturbed prompts remain the same. As a result, any fluctuation in answers of LMM directly reflects its uncertainty. On the other hand, semantic-inequivalent perturbation alters the original semantics, and changes in the answers are inevitable, making it difficult to accurately reflect the inherent uncertainty of the LMM.

Why is prompt perturbation superior to vanilla sampling for capturing LMM uncertainty? Multimodal prompt perturbation challenges the LMM with prompts that vary at different levels, with larger variations of answers indicating higher uncertainty. In contrast, vanilla sampling typically uses a high temperature during sampling, which tends to induce high uncertainty across all samples. For instance, the LMM could be highly confident in its answer, but the high temperature inevitably causes answer variation, leading to an artificially high uncertainty.

Can multimodal semantic uncertainty extend to more modalities? Yes. Uncertainty-o proposes a general pipeline for LMM uncertainty estimation. This pipeline is orthogonal to and can benefit from iterations of LMM. With a more general LMM, which is capable of parsing the semantic content of additional modalities into textual descriptions, Uncertainty-o can seamlessly estimate uncertainty for those answers in more modalities.

Why not directly utilize LMM to check whether two generated multimodal responses are semantically equivalent? Current LMMs still lack proficient ability for multimodal semantic checking. We have attempted two methods to utilize LMM for direct multimodal data semantic checking: (1) Combine two multimodal answers into one and prompt the LMM to check whether the answers are similar. For example, merge two point clouds into one and conduct shifting so that they do not overlap. However, current LMMs show unsatisfactory performance. (2) Directly input two answers into LMM and prompt it to check. We find that many LMMs still do not support multi-input, such as understanding two point clouds simultaneously.

7. Setting

Benchmark. We conduct experiments with 18 benchmarks. For the comprehension hallucination task, the benchmarks we adopt are typically QA-type. For images, we utilize

MMVet, LLaVABench, and CoCoCap. For video benchmarks, we leverage MSRVTQA, MSVDQA, and NextQA. For the audio modality, we use ClothV2 and AudioCaps. For point cloud benchmarks, we utilize PointCap and ModelNet. For generation hallucination detection, we use caption-type benchmarks and employ captions as generation prompts. For image generation, we utilize Flickr. For video generation, we utilize MSRVT. For audio generation, we utilize VCTK. For point cloud generation, we utilize Pix3D, aiming for image-to-point cloud generation. For the safety-critical task, we utilize MIMIC-CXR and OpenEQA. MIMIC-CXR is a benchmark of chest X-ray images annotated with medical diagnoses by radiologists. OpenEQA is an in-house video benchmark from an embodied robot’s perspective, accompanied by text-based questions.

LMM. We experiment with 10 different LMMs capable of understanding and generating various modalities of data. For closed-source LMMs, we utilize GPT-4o and QwenVL-Max. For open-source LMMs, InternVL is a large vision-language model that takes image-text prompts and answers with text. VideoLLaMA takes videos as prompts and generates text answers. OneLLM is proficient in processing various modal inputs, *e.g.*, audio and point clouds, and outputs text-only responses. PointLLM is specifically designed for real-world point cloud understanding. StableDiffusion serves as a text-based image generation model. VideoFusion is an efficient video generation model, taking text as a prompt. AnyGPT is capable of generating audio and visual data. RGB2point realizes point cloud generation by taking a single image.

Implementation Details. The hallucination detection procedure contains 3 key phases: (1) Initial answer obtaining. The tested LMM is first given the context to generate an initial output. We keep the variation hyper-parameter low at this stage, *e.g.*, low temperature for LLM-based large models and high guidance scale for Diffusion models. The initial answer is compared with the ground truth to decide whether it contains hallucinations. (2) Uncertainty estimation. Initial contexts are perturbed by our proposed multimodal prompt perturbation, according to the modalities they contain. All modal prompts are perturbed simultaneously to various degrees. Different levels of perturbed prompts enable the sampling process. For sampled textual answers, an off-the-shelf LLM, Qwen2.5-7B, clusters them by semantics and calculates entropy as uncertainty. For other modalities’ answers, *e.g.*, images, we use OneLLM-7B as

Text Clustering	AUROC↑	AURAC↑	ECE↓
Lexical	48.0	33.2	12.7
Semantic	55.4	39.2	10.8

Table 10. **Ablation of Text Clustering.** During semantic uncertainty calculation, clustering based on semantics is more effective than clustering based merely on lexical presentation.

Method	AUROC↑	AURAC↑	ECE↓
Cycle Consistency	57.7	72.9	9.2
Uncertainty-o	59.5	74.5	8.3

Table 11. **Ablation of Cycle Consistency for Generation Hallucination Detection.** Uncertainty-o surpasses cycle consistency, as cycle consistency is constrained by the text similarity scoring capability of the LLM. We experiment on Flickr with StableDiffusion.

a captioner to convert those answers into concise captions. Then, the uncertainty calculation is simplified to vanilla textual semantic uncertainty. (3) Hallucination detection. With hallucination labels from (1) and estimated uncertainties from (2), we utilize AUROC, AURAC, and ECE as hallucination detection metrics. These three metrics comprehensively evaluate the calibration degree between uncertainties and hallucinations. For hallucination mitigation, we follow a two-stage procedure: (1) We first prompt the LMM with initial context to obtain an initial answer and calculate its uncertainty using Uncertainty-o. (2) We then select the top 50% of answers with the highest uncertainty, as these are most likely to contain hallucinations. For each of these answers, we utilize the following prompt: ‘Prompt: \$X, Initial Answer: \$Y, Your answer has a high uncertainty score of \$U, which ranges from 0 to 1. Could you improve your answer and revise it to be more accurate? \$X, \$Y, and \$U refer to the actual content of original prompt, initial answer and estimated uncertainty. Finally, we use the revised answer as the final output from the LMM. For uncertainty-aware CoT, we treat it as a multi-round thinking process. In the first round, we append the original prompt with ‘Let’s think step-by-step. Now, provide your first step of the answer.’ We then estimate the LMM uncertainty with Uncertainty-o. From the second step onward, in addition to the original prompt, we append all previous answers and their corresponding uncertainty scores. At the end of the prompt, we add ‘Respond with ‘Finish.’ when you think you have solved the question.’ We check answer at every step for the presence of ‘Finish.’ and exit the loop once we find it.

8. More Ablations

Text Clustering Manner. We report the ablation of text clustering methods (see Tab. 10). Clustering text based on its inherent semantics, rather than merely its lexical presentation, yields the best results.

Cycle Consistency. We also experiment with cycle consistency for detecting hallucinations in image generation settings (see Tab. 11). We observe that Uncertainty-o surpasses this baseline method, which is limited by the scoring ability of the LLM for text pair similarity.

9. Detailed Proof for Proportional Theorem

9.1. Definitions and Assumptions

- Sampling Process:** The large model M give predictions concurrently for perturbed prompts x_i and x_j . For those input prompts, the predictions from the large model is $y_i = M(x_i)$, and $y_j = M(x_j)$, respectively.
- Uncertainty:** We focus on the large model’s *Epistemic Uncertainty*, which is the uncertainty in the large model parameters. Assume the large model parameters θ are random variables with a prior distribution $P(\theta)$.
- Prediction Difference:** Define the prediction difference $D(x)$ as:

$$D(x) = \|y_i - y_j\|,$$

where $\|\cdot\|$ denotes semantic space distance.

9.2. Mathematical Derivation

Large Model’s Predictive Distribution. Assume the large model’s output is a probability distribution $P(y|x, \theta)$, where y is the response, x is the prompt, and θ are the model parameters.

Posterior Predictive Distribution. According to Bayes’ theorem, the posterior predictive distribution of the large model can be expressed as:

$$P(y|x) = \int P(y|x, \theta)P(\theta|x)d\theta,$$

where $P(\theta|x)$ is the posterior distribution of the large model parameters.

Epistemic Uncertainty. The uncertainty in the parameters can be measured by the variance of the posterior distribution:

$$\text{Var}(\theta|x) = \mathbb{E}_{\theta|x}[(\theta - \mathbb{E}_{\theta|x}[\theta])^2] = \mathbb{E}_{\theta|x}[\theta^2] - (\mathbb{E}_{\theta|x}[\theta])^2.$$

Prediction Difference and Epistemic Uncertainty. To relate the prediction difference $D(x)$ to parameter uncertainty, we need to consider the predictions from the perturbed prompts. Assume the parameters during i -th and j -th prompt perturbation are θ_i and θ_j , respectively, and they have the same prior distribution, i.e., $P(\theta_i) = P(\theta_j)$.

Predictions from Perturbed Prompts. The predictions from perturbed prompts can be expressed as:

$$y_i = \mathbb{E}_{\theta_i|x} [P(y|x, \theta_i)],$$

$$y_j = \mathbb{E}_{\theta_j|x} [P(y|x, \theta_j)].$$

Expression for Prediction Difference. Assume the difference in predictions can be approximated by a First-order Taylor Expansion:

$$y_i - y_j \approx \mathbb{E}_{\theta|x} [\nabla_{\theta} P(y|x, \theta) \cdot (\theta_i - \theta_j)],$$

where $\nabla_{\theta} P(y|x, \theta)$ is the gradient of $P(y|x, \theta)$ with respect to θ .

Thus, the prediction difference $D(x)$ can be expressed as:

$$D(x) = \|y_i - y_j\| \approx \mathbb{E}_{\theta|x} [\|\nabla_{\theta} P(y|x, \theta) \cdot (\theta_i - \theta_j)\|].$$

Relationship Between Prediction Difference from Prompt Perturbation and Epistemic Uncertainty. To simplify the analysis, assume θ_i and θ_j are independently and identically distributed (i.i.d.). Then:

$$\mathbb{E}_{\theta|x} [\|\nabla_{\theta} P(y|x, \theta) \cdot (\theta_i - \theta_j)\|^2] \approx$$

$$\mathbb{E}_{\theta|x} [\|\nabla_{\theta} P(y|x, \theta)\|^2] \cdot \mathbb{E}_{\theta|x} [(\theta_i - \theta_j)^2].$$

With $\mathbb{E}_{\theta|x} [(\theta_i - \theta_j)^2] = 2 (\mathbb{E}_{\theta|x} [\theta^2] - (\mathbb{E}_{\theta|x} [\theta])^2) = 2 \cdot \text{Var}(\theta|x)$, we have:

$$\mathbb{E}_{\theta|x} [\|\nabla_{\theta} P(y|x, \theta) \cdot (\theta_i - \theta_j)\|^2] \approx$$

$$2 \cdot \mathbb{E}_{\theta|x} [\|\nabla_{\theta} P(y|x, \theta)\|^2] \cdot \text{Var}(\theta|x).$$

Assuming $k = \mathbb{E}_{\theta|x} [\|\nabla_{\theta} P(y|x, \theta)\|^2]$, which is positive, we get:

$$\mathbb{E}_{\theta|x} [\|\nabla_{\theta} P(y|x, \theta) \cdot (\theta_i - \theta_j)\|^2] \approx 2k \cdot \text{Var}(\theta|x).$$

Thus, the prediction difference $D(x)$ from prompt perturbation can be expressed as:

$$D(x) \approx \sqrt{2k} \cdot \sqrt{\text{Var}(\theta|x)}.$$

Simplifying further, we obtain:

$$D(x) \propto \sqrt{\text{Var}(\theta|x)}.$$

9.3. Final Theorem

From the above derivation, we have shown that the prediction difference $D(x)$ from prompt perturbation is proportional to the square root of the model's epistemic uncertainty $\sqrt{\text{Var}(\theta|x)}$. Therefore, the prediction difference $D(x)$ can serve as a measure of the model's epistemic uncertainty for a given sample.